Transactions on Engineering Sciences vol 43, © 2003 WIT Press, www.witpress.com, ISSN 1743-3533

Modeling multiphase flow of liquefied removable epoxy foam

A.C. Sun[1], K.L. Erickson[1], M.L. Hobbs[1], D. Adolf[2] & M. Stavig[2]
[1]*Engineering Sciences Center, Sandia National Laboratories, USA*
[2]*Materials and Process Sciences Center, Sandia National Laboratories, USA*

Abstract

Removable epoxy foam (REF) has been considered for the redesign of engineering systems. The response of REF in an intense thermal environment is part of the material response program within the Engineering Sciences Center. More specifically, this paper addresses liquefaction of REF during foam pyrolysis under moderate to high pressures. Understanding the liquefaction process and modeling of the liquid flow are essential to ensuring the performance of the new design. The phase transition from solid to liquid to vapor is the result of heat transfer, mass transfer, decomposition chemistry, and phase equilibria. Fluid phase thermophysical property measurements and predictions are necessary for modeling the flow. We have obtained thermal conductivities of REF up to 200C; extrapolation to higher temperature is necessary for liquid phase model. Viscometric measurements have been attempted at 80C and 180C. The observed stress of foam at 180C under constant strain rate shows non-asymtotic behavior, suggesting a continuous changes in the polymer structure. The modeling of liquid flow is based on a 2D geometry and solved by a finite-element code. In the model, liquid and solid phases deform under coupled decomposition kinetics, energy, momentum, and mass balances. The moving boundaries are controlled by a set of distinguishing conditions at the interfaces between solid and liquid and liquid and vapor. Preliminary results of the liquefaction model will be discussed.

1 Introduction

Once an epoxy-based foam was identified as the replacement foam for engineering systems at Sandia National Laboratories, work was begun to understand its thermal, chemical, and mechanical response to abnormal thermal environments, such as fire. The term "removable" stems from a desirable feature in this material. Solid REF becomes soluble in mild organic solvent when heated to 90C. This functionality is intended to provide ease of removing the foam for maintaining/reworking the system [1].

Experimentally, thermal-gravimetric analysis (TGA) of small foam samples (2-5mg) is used to understand the basic chemical reaction mechanisms during thermal degradation of the foam. In addition, x-ray images of larger foam samples (8.8-cm diameter, 14.6-cm high cylinders) subjected to a radiant heat source at different orientations have been recorded. In both techniques, samples of REF are heated from ambient to either 750C or 900C [2].

In the past, liquefaction of the foam was considered negligible for modeling unconfined burning of polyurethane foam [3]. This becomes inadequate when considering REF. As shown in Figure 1, based on the x-ray image analysis of a single top-heated experiment, up to 10% by volume of liquefied REF is believed to exist during thermal pyrolysis. Furthermore, the existence of a flowing medium inside an engineering system may yield unexpected overall behavior.

The objective of this work is then to construct a numerical model that addresses the importance of the fluid phase to the overall material response of REF. Other than solving for energy balance, the model will include mass and momentum transfer to account for the flowing medium. The resulting partial differential equations are solved using a finite-element code developed within the Engineering Sciences Center.

The next section briefly describes the decomposition kinetics and thermophysical properties of REF. This is followed by a description of the finite-element model for tracking thermal decomposition and fluid flow of REF along with some preliminary results.

2 Material characterization of removable epoxy foam

2.1 Decomposition chemistry of REF

REF decomposition chemistry differs significantly from its synthesis. The major thermodynamic driving force when a encapsulated foam undergoes heating is thermal conduction and radiation. Analysis of off-gas from the TGA experiments yields information about the chemical constituents likely present in the liquid phase, but resolving the exact chemistry responsible for decomposition and phase transition is extremely difficult. An initial off-gas study indicates three decomposition regimes [4]. For temperatures ranging from room to 140°C, the loss of mass is due to loss of blowing agent and surfactant. Between 140°C and 300°C, polymeric forms of siloxane and some small organic compounds (e.g. 2-furanmethanol) continue to evolve. In this temperature range, the foam undergoes significant physical changes as decomposition products evolve into gas. Figure 2 compares the physical appearance of non-

porous REF at room, 208°C, and 241°C (non-porous REF is defined as a REF without its blowing agent). Above 300°C, heavier components such as bisphenol-A, toluene, and phenol have all been observed in the off-gas.

While we believe that there is a strong pressure dependency to the amount or the rate of liquefaction, there has not been a single experiment that can quantify the extent. The mass loss is delayed compared to atmospheric TGA analysis when pressure is increased, indicating a delay in volatilization due to thermodynamic shifts. The confinement of the sample also results in the same shift in TGA curves, indicating a strong dependency in mass transfer resistance. Recent experiments have also been devoted to understanding pressure dependency on thermal decomposition. In a totally-confined foam sample, pressure as high as 34 bar has been recorded.

Thus far, simple as well as complex kinetics models with parameters fitted from TGA experiments have been constructed. This methodology is analogous to the one described by Hobbs [5]. In this study, chemical decomposition is represented by a two-step, first-order kinetics model.

$$F \xrightarrow{k_1} 0.3G_1 + 0.7P \tag{1}$$

$$P \xrightarrow{k_2} 0.943G_2 + 0.057S \tag{2}$$

$$r_1 = k_1[F], \quad r_2 = k_2[P], \quad k_i = A_i \exp\left(\frac{-E_i}{RT}\right), \quad i = 1,2 \tag{3}$$

F, P, and S are mass fractions of foam, primary product, and carbonaceous residue. G_1 and G_2 are initial off-gas and secondary gas products. Although simplistic, the first reaction dominates in the lower temperature range, which is representative of the initial off-gas from the blowing agent and siloxanes. The product, P, can be viewed as the species that exist in fluid-like phase ranging from a mixed bubbly froth layer to a rubbery solid. It peaks at around 300° C and is further degraded into mostly gas, G_2 and a small amount of carbonaceous residue. The Arrehnius parameters A_i and E_i are obtained by fitting low-pressure TGA results. No pressure dependency exists in the current form of the kinetics model. Reaction calorimetry is also used to characterize the heat of reaction during decomposition. Total heat of reaction is believed to be on the order of 100 cal/gm (endothermic).

2.2 Thermophysical properties of REF

As eluded to earlier, thermal conduction is one of the dominant driving forces; hence, the numerical model relies on an accurate description of the thermal conductivity. Experiments to measure temperature dependency of thermal conductivity have been carried out both inhouse and externally. Because REF is evolving into a different material with large volume and composition changes, the measurements have been limited to 195°C using non-porous samples. Table 1 lists the temperature dependency of thermal conductitivity based on heated probe method [6]. The thermal conductivity increases slightly before it decreases starting from 150°C. The decrease at higher temperature may be due to the reactions occurring at higher temperature. Extrapolation to a higher

temperature is needed in order to model thermal behavior of REF in the higher temperature regime. Final values of thermal conductivity for porous REF are calculated by adding the contribution from the closed cells.

Viscometric measurements for REF have been attempted to understand the viscoelastic behavior of the polymer at high temperature. The non-porous REF is subjected to dynamic mechanical analysis. Figure 3 is a plot of shear modulus versus time for REF at 80° and 180°C (T_g for REF is 70°C) subjected to a step change in strain. At those temperatures, no indication of fluid-like behavior is observed. The modulus continues to decrease as a function of time indicating continuous changes in the material structure. Stress under constant strain rate is also measured at 180 °C. The transient response of the stress does not approach an equilibrium value, indicating a solid-like material at that temperature. As mentioned before, because significant changes are observed visually with the material, any meaningful viscometric measurement seems intractable. We also believe that fluid-like behavior is more pronounced under pressurized conditions, and such a set up is under consideration.

3 Multiphase model of REF thermal decomposition

3.1 Top-heated scenario

In order to simulate liquefaction fully, chemical kinetics as well as the phase transitions must be handled properly. The size of the liquid domain is bounded by the solid-liquid and liquid-vapor interfaces and is dependent upon temperature and pressure. Consider a top-heated foam encapsulated in a stainless-steel cylindrical can as shown in Figure 4. In this heating orientation, foam recession due to decomposition occurs in an axisymmetric manner such that a two-dimensional model can be assumed. The element mesh of the numerical model is also shown. Two distinct finite-element mesh domains indicate solid and liquid phases. Gas phase domain is ignored for the simplicity of the model. This does not preclude the mass transfer resistance in the gas phase, which can be solved as a boundary condition for the liquid phase. In addition, the pressure information is not lost by this assumption, the impact of convective gas transport, and radiation enclosure calculations is sacrificed by modeling only solid and fluid phases. The governing equations in each phase and their associated boundary conditions are set up and solved using an internally developed finite-element code. The program solves coupled mass, momentum, and heat transfer with specialization in moving boundaries [7]. In the next three subsections, the numerical model is described in more details.

3.1.1 Fluid domain

Because the condensed phase consists of reactive liquid, explicit mass, energy, and momentum balances are solved for this phase.

$$\rho \frac{dv}{dt} = -\rho(v - v_m)\cdot\nabla v - \nabla p + \nabla\cdot(\mu(\nabla v + \nabla v^T)) + g \tag{4}$$

$$\nabla \cdot T_s = 0 \tag{5}$$

$$\frac{d(\rho C_p T)}{dt} = (v - v_m)\cdot\nabla(\rho C_p T) - \nabla\cdot q + H_{rxn} \tag{6}$$

$$\frac{dy_i}{dt} = (v - v_m)\cdot\nabla y_i - \nabla\cdot J_i + r_i, \quad i = 1,2,3 \tag{7}$$

$$\nabla\cdot v = \sum_i \rho_i r_i, \quad i = 1,2,3 \tag{8}$$

Eqn. (4) is the liquid phase momentum equation, where $\boldsymbol{v}$ is the fluid velocigy, $\boldsymbol{v}_m$ is the mesh velocity, p the pressure, and $\boldsymbol{g}$ the gravitational force. The mesh velocity is defined as the time derivative of the nodal displacement and solved as an pseudo-elastic solid using pseudo-solid stress balance, Eqn. (5), where $\boldsymbol{T}_s$ is the solid stress. The shape of the boundaries is then tracked by a set of distinguishing conditions [8].

Eqn. (6) is the energy balance for the liquid phase. $\boldsymbol{q}$ is the heat flux vector. H_{rxn} is the latent heat required for the reactions. Eqn. (7) is the component mass balance, which contains the convective-diffusion portion as well as a reaction source. y_i is defined as the mass fraction of either F, P, or G=G_1+G_2. Eqn. (8) is the continuity equation for the domain with a volumetric mass source due to density variations. ρ_i is the inverse of specific volume of component i. Since mass fraction of S is not an independent variable (i.e., $y_s = 1 - \sum_i y_i$), its mass balance is not solved. It is expected that local density difference due to concentration gradient will initiate convective mixing in this phase.

3.1.2 Solid domain

In the solid phase, the equations of interest are energy and mesh equations, namely, Eqns (5) and (6). No flow is necessary to solve in this phase. The speed at which the solid-fluid interface moves is controlled by the boundary conditions specified for that interface. The demarcation of the solid-fluid phase boundary becomes more arbitrary and the details are explained in the next section.

3.1.3 Boundary conditions

Each boundary, defined by the interface shared by two or more element domains, can either be a solid boundary (e.g. pipe wall) or a phase boundary (e.g. liquid-vapor or solid-liquid interface). The finite-element program requires a set of distinguishing conditions to tie the motion of the mesh to the physics at the interface. Since the onset of liquefaction cannot be inferred from the TGA data (as well as the simple kinetics model), we are using an isotherm of 90°C to be the distinguishing condition for the mesh equation at the solid-fluid interface, Eqn. (9). In other words, the interfacial boundary follows the movement of temperature. It is very important to note that this is not a physical melting boundary but merely a numerical demarcation. The fluid velocity $\boldsymbol{v}$, not the boundary velocity, is set to be zero at the boundary, as defined in Eqn. (11). The boundary conditions for the components are set at what the reactant and product

concentrations are at 90°C; i.e., $1 - y_F = 0.08,\ y_P = 0.055,\ and\ y = 0.024.$ This is reflected in Eqn. (10)

$$T - T_o = 0 \tag{9}$$

$$y_i - y_o = 0, \quad i = 1,2,3 \tag{10}$$

$$v = 0 \tag{11}$$

At the fluid-vapor interface, recession of the foam is controlled by the mass transfer of liquefied foam into gas phase, which is a function of temperature and pressure. An effective mass transfer rate can be applied at that boundary.

$$\boldsymbol{n} \bullet \boldsymbol{J}_i + \boldsymbol{n} \bullet (\boldsymbol{v} - \boldsymbol{v}_m) y_i = k_i (y_i - y_i^{gas}), \quad i = 1,2,3. \tag{12}$$

The right hand side describes the mass transfer resistance into the vapor phase. The boundary condition for the temperature is satisfied by applying a constant heat flux as prescribed in the experiment. The velocity at the interface will be satisfied via a surface tension condition. A balance of the viscous stress with the capillary stresses at the interface defines the shape of the meniscus. While the gas-liquid interface in the experiments show some degree of frothing, the model reduces it to a single boundary. For the mesh equation, the speed of the mesh at the interface is controlled by the overall mass loss due to evaporation.

$$n \bullet (v - v_m) = \sum_i k_i (y_i - y_i^{gas}) \tag{13}$$

Figure 4 shows the experimental and simulation results of a top-heated foam block when the foam has recessed half way. The comparison between the experiment and the simulation is currently qualitative, as the rate of evaporation does not match the rate observed in the experiment. The mass transfer coefficient for the total gas component can be varied to match the experimental data. The amount of fluid increases as the density decreases in the liquid phase. The specific volume of each component is estimated currently.

3.2 Side-heated scenario

The most observable impact that the fluid has on the overall heat transfer characteristics is when the foam is heated from the side. Figure 5 shows the snapshot of the experiment for this problem. Note that the solid-fluid boundary has been removed from this set up in order to eliminate tracking two moving boundaries. This means that the entire domain is being treated like a fluid with viscosity function that starts as solid-like material at room temperature to fluid-like material. The degree of freedom for this problem is also much larger than the top-heated model, since all of the fluid, species, and energy equations are solved throughout the domain (i.e., Eqns. (4) to (8)).

Figure 5 also shows the simulation results of 2D side-heated simulations. The liquid and vapor boundary is distorted due to the gravitational force. The shape of the boundary is sensitive to viscosity of the foam as well as the mass transfer coefficient of the component. In both cases, the viscosity is a function of temperature.

$$\mu(T) = \mu^{o} \exp\left(\frac{-E}{RT}\right) \tag{14}$$

μ^{o} is the nominal viscosity value for the foam. The results from Figure 5 are based on μ^{o} of 10 cp and E of 5600 call/mol.

Because numerical convergence is very sensitive to the sharp energy (and therefore mass) gradients at the fluid-vapor interface and because remeshing is required after large mesh distortion, there are computational challenges to overcome in modeling foam liquefaction in 2D and 3D geometries. Currently, mesh refinement is necessary near the vapor-liquid interface in order to achieve convergence. This problem is similar to the one encountered in the thermal model [5]. When the mesh becomes distorted, remesh-remap is required to restart the simulation. This is one of the drawbacks of the current algorithm. We are currently investigating a level-set based technique to track the interface.

4 Acknowledgements

Sandia is a multiprogram laboratory operated by Sandia Corporation, a Lockheed Martin Company, for the United States Department of Energy under Contract DE-AC04-94AL85000. The authors would like to thank Tom Baer, Andy Kraynik, Walt Gill for providing guidance on this work. In addition, we would like to acknowledge Ed Russick for providing non-porous REF and Kyle Thompson for the x-ray images.

References

[1] Aubert, J.R., McElhanon, J.R., Saunders, R.S., Sawyer, P.S., Wheeler, D.R., Russick, E.M., Rand, P.B., & Loy, D.A., "Progress in Developing Removable Foams, Adhesives, and conformal coatings for the encapsulation of weapon components," Internal Sandia Report SAND2001-0295.

[2] Erickson, K.L., Truijillo, S.M., Thompson, K.R., Sun, A.C., Hobbs, M.L., & Dowding, K.J., :Liquefaction and flow behaviour of a thermally decomposing removable epoxy foam," Proceedings to 2nd International Conference on Computational Methods in Multiphase Flow, 2003.

[3] Erickson, K.L., Borek, T. T., & Renlund, A. M., Chu, T. Y., Hobbs, M.L., Clayton, D., & Fletcher, T.H., "Thermal decomposition of rigid polymeric foams: experimental and modeling Issues", Fourth Biennial Tri-Laboratory Engineering Conference on Modeling and Simulation, October, 2001.

[4] K. L. Erickson, "Thermal decomposition products from removable epoxy foam (REF)," Sandia Internal Memo, February, 2002.

[5] M. L. Hobbs and G.H. Lemmon, "Polyurethane foam response to high heat flux," Proceedings to 2nd International Conference on Computational Methods in Multiphase Flow, 2003.

[6] Gembarovic, J. & Taylor, R.E., "Thermophysical Properties of Plastic Sample: A report to Sandia National Laboratories," Thermophysical Properties Research Laborabory Report 2868, 2002.

[7] Schunk, P.R., Sackinger, P.A., Rao, R. R., Chen, K. S., Baer, T.A., Labreche, D. A., Sun, A. C., Hopkins, M. M., Subia, S. R., Moffat, H. K., Secor, R. B., Roach, R. A., Wilkes, E. D., Noble, D. R., Hopkins, P. L., & Notz, P. K., "GOMA 4.0 – A Full-Newton Finite Element Program for Free and Moving Boundary Problems with Coupled Fluid/Solid Momentum, Energy, Mass, and Chemical Species Transport: User's Guide," Sandia Report, SAND2002-3204, 2002.

[8] Sackinger, P.A., Schunk, P.R., and Rao, R.R., "A Newton-Raphson Pseudo-Solid Domain Mapping Technique for Free and Moving Boundary Problems: A Finite Element Implementation," *J. of Computational Physics*, **125**, 83-103, 1996.

Table 1 – Thermal conductivity of non-porous REF (REF108).

Temperature, (°C)	k, (W cm^{-1} K^{-1})
23.0	0.00176
82.0	0.00183
130.0	0.00184
150.0	0.00165
175.0	0.00146
194.0	0.00110

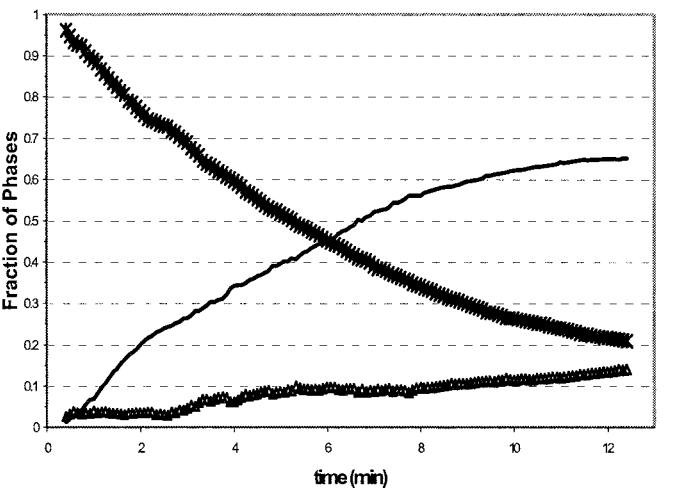

Figure 1 – Phase fraction for top-heated REF experiment 20 as a function of time. Cross = solid fraction; line = gas fraction; triangle=liquid fraction.

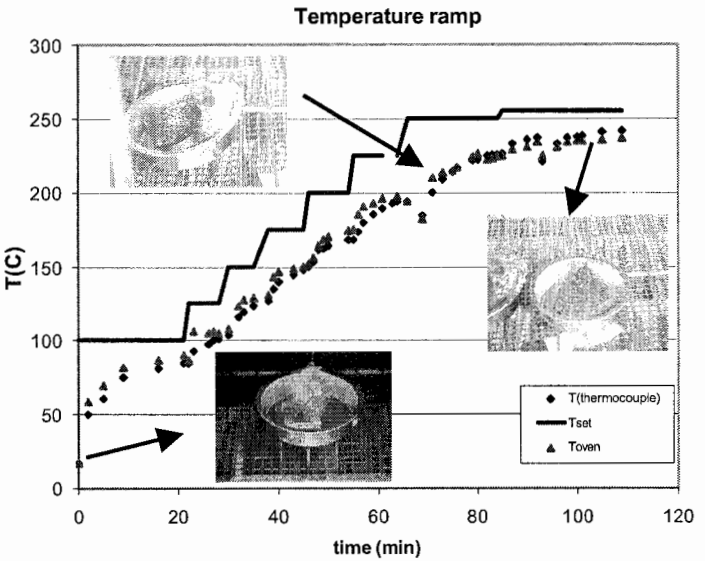

Figure 2 – Images of nonporous-REF (REF108) at room temperature, 208°C, and 241°C.

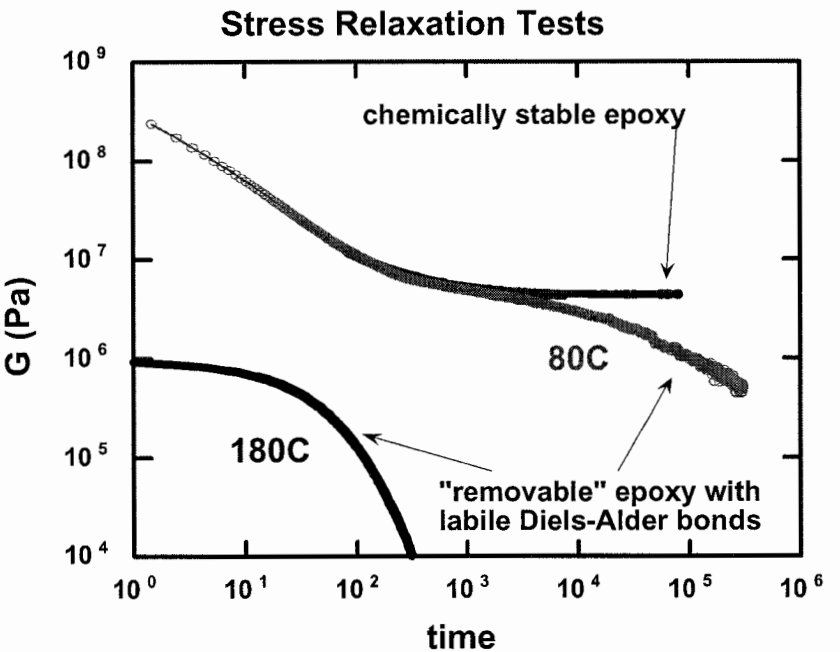

Figure 3 – Viscometric measurement of REF at different temperatures. Shear modulus does not reach an equilibrium value and suggests dynamic changes in solid foam structure.

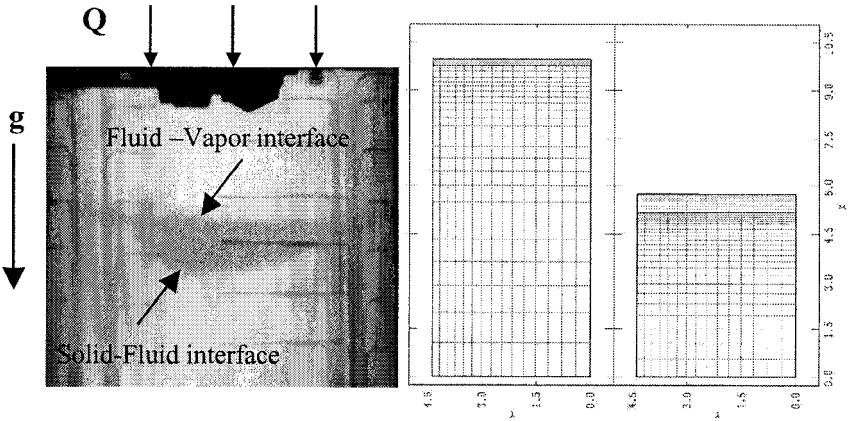

Figure 4 – Top heated foam experiment (REF 20, 2bar) and GOMA simulation. Foam encapsulated in a can is heated from the top. The dark dense region is believed to be liquefaction zone. Simulation contains two domains, the solid and liquid.

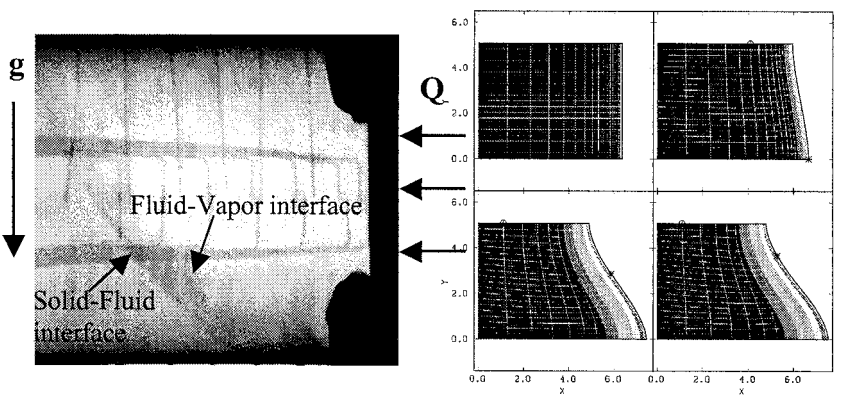

Figure 5 – Side-heated experiment and simulation. The experimental image (REF8) shows liquefied product flowing down to the bottom of the can. GOMA simulation showing contours of y_P, mass fraction of intermediate component.